Colloid Polym Sci 275:1148–1155 (1997)

ORIGINAL CONTRIBUTION

J.A. Maroto
F.J. de las Nieves

Estimation of kinetic rate constants by turbidity and nephelometry techniques in a homocoagulation process with different model colloids

Received: 2 June 1997
Accepted: 14 August 1997

F.J. de las Nieves (✉)
Group of Complex Fluids Physics
Department of Applied Physics
University of Almería
04120 Almería
Spain

J.A. Maroto
Department of Applied Physics
Polytechnique School
University of Jaén
23700 Linares, Jaén
Spain

Abstract In this work turbidimetric and nephelometric techniques have been used to study the homocoagulation of aqueous dispersions of uniform spherical particles of surfactant-free latexes. Cationic and anionic latexes of similar particle sizes (361 and 370 nm) and different surface charge densities (+16.4 and −3.6 $\mu C/cm^2$) were used throughout. The kinetic constants which control the aggregation processes when the electrical repulsion disappears were estimated by both techniques at different particle concentration and wavelength in order to establish the experimental conditions which provided reliable and similar values for the coagulation rate constant. Both experimental techniques (turbidity and nephelometry) and two ways of fitting the data have been used with both latexes. For the first method, the initial slope of turbidity or total scattered intensity versus time curves were used to calculate the kinetic constants. In the second method, the whole turbidity or total scattered intensity versus time curves were fitted and the kinetic constants calculated. An unambiguous experimental value for the doublet rate constant in diffusion conditions is obtained by turbidity and nephelometry techniques. By nephelometry both data treatments have permitted a distinction between the doublet rate constant and the global rate constant in diffusion conditions.

Key words Colloid stability – polymer colloids – turbidity – nephelometry

Introduction

A colloidal dispersion is never thermodynamically stable. The total free energy of a dispersed system can always be lowered by reduction of the interfacial area, that is, by a coagulation process. The reduction in the rate of coagulation is due to the formation of an electrical double layer at the particle–liquid interface [1, 2]. However, when two particles approach one another their double layers interact giving rise, in certain conditions, to repulsive forces which prevent coagulation.

The mechanisms and kinetics of the coagulation of colloidal particles have been investigated experimentally, theoretically, and using simulation. The principal interest of the stability and kinetics of coagulation of colloidal particles in liquids resides in the practical applications. Examples include synthesis of engineering ceramics [3, 4], particulate separation processes, such as flotation and selective flocculation [5], manufacturing of pharmaceutical [6, 7] and biomedical products [6, 8–10], and other industrial process such as "structuring" of agricultural pesticides or soil conditions [6].

Coagulation kinetics have been studied by a wide variety of techniques. Direct counting of the coagulating colloids using an ultramicroscope [11], using a particle counter [11–13] or using the single-particle optical sizing (SPOS) technique [14]. Another common method is to

monitor changes in the turbidity of the coagulating suspension with time [15–17]. Finally, we mention the dynamic light scattering [18–21], total intensity light scattering [22–24] and multiangle scattered light methods [25].

The total intensity light scattering method (nephelometry) and the optical absorbance are the most simple techniques to study the coagulation process and it is possible to use them in the majority of laboratories. For nephelometry the main disadvantage is the necessity of using a single low angle for runs, which implies problems with dust contamination [23] and thus may not provide accurate values of coagulation rates. On the other hand, if we use larger diffusion angles, as in this work, we eliminate this inconvenience but we must hypothesize about the adequate form factors [22] that characterize the aggregates.

In this work we use turbidimetric and nephelometric techniques to study the homocoagulation of aqueous dispersions of uniform spherical particles of surfactant-free cationic and anionic latexes. The use of particles with opposite signs of their surface charge is of special interest in heterocoagulation processes, when both type of particles are in dispersion at the same time and the driving force for the aggregation process is the electrostatic interaction. As a first step, however, it is necessary to study the coagulation of each latex and to establish the kinetic constants which control their aggregation processes when the electrical repulsion disappears. Looking for this objective, we have obtained the experimental stability factor (W) and the fast coagulation rate constants for both systems. Owing to the variety of experimental results reported in the literature [26], the major effort has centred on obtaining reliable and similar values for the coagulation rate constant. For these reasons two experimental techniques (turbidity and nephelometry) and two ways of fitting the data have been used with both latexes. It has been possible to establish the methodology and experimental conditions which provide similar kinetic constants for both latexes using both techniques.

Theory

Turbidimetry

Classically, the initial slope of the absorbance versus time curve is the quantity obtained in these runs. The stability factor (W), defined as the ratio of the fast and slow doublet rate constant, can be evaluated in turbidimetry by relating the initial slopes in fast and slow aggregation processes:

$$W = \frac{(\mathrm{d}\tau/\mathrm{d}t)_{0,\mathrm{F}}}{(\mathrm{d}\tau/\mathrm{d}t)_{0,\mathrm{S}}}, \tag{1}$$

in which τ is the turbidity, t the time and the subscripts F and S refer to a fast or slow experience.

Also, it is feasible to evaluate the absolute rate constant if we select a suitable particle number in the cell and also the wavelength [16, 17]:

$$\left(\frac{\mathrm{d}\tau}{\mathrm{d}t}\right)_0 = \left(\frac{1}{2}C_2 - C_1\right)K_{\mathrm{D}}N_0^2, \tag{2}$$

where C_2 and C_1 are the scattering sections of the doublet and singlet, respectively, N_0 is the initial number of singlets in the cell and K_{D} is the doublet rate constant, defined from the coagulation kinetics equation [11] for conditions of zero time:

$$\frac{\mathrm{d}N_0}{\mathrm{d}t} = -K_{\mathrm{D}}N_0^2 . \tag{3}$$

There are also recent studies that, by analogy with nephelometric experiments, treat the whole of the $A(t)$ curve [27, 28]. So, we can write the absorbance function versus time, $A(t)$, in a polynomial form [27], valid for initial times as

$$A(t) = a + bt + ct^2 , \tag{4}$$

where a, b and c are constants and can be expressed as

$$a = 4.342 \times 10^{-3} N_0 C_1 , \tag{5}$$

$$b = 4.342 \times 10^{-3} K_{\mathrm{D}} N_0^2 (C_2 - 2C_1) , \tag{6}$$

$$c = 1.30 \times 10^{-2} K_{\mathrm{D}}^2 N_0^3 (C_1 + C_2) . \tag{7}$$

Nephelometry

Previous works [23, 29] have established the validity of the equation:

$$I_j(\theta) = jI_i(\theta)\left[1 + \left(\frac{2}{j}\right)A(j,\theta)\right], \tag{8}$$

where $I_j(\theta)$ is the intensity of light scattered at an angle θ by a j-fold aggregate of monodisperse spheres and $I_1(\theta)$ the corresponding single-sphere Mie intensity. $A(j,\theta)$ is a geometry factor given by

$$A(j,\theta) = \sum_{i=1}^{j-1}\sum_{k=i+1}^{j} \frac{\sin[(4\pi n_2 h_{ik}/\lambda)\sin\theta/2]}{[(4\pi n_2 h_{ik}/\lambda)\sin\theta/2]} , \tag{9}$$

where h_{ik} is the distance between centers of the ith and jth particle in the aggregate, λ the wavelength of incident light in vacuo and n_2 the refractive index of the dispersion medium.

Now we can consider the intensity of light scattered at an angle θ by the whole colloidal dispersion:

$$I_\theta(E) = \sum_{j=1}^{\infty} N_j(E) I_j(\theta) , \tag{10}$$

where $N_j(E)$ is the number concentration of an aggregate of j particles at reduced time $E = t/t_{1/2}$ such that

$$t_{1/2} = \frac{1}{KN_0} = \frac{t}{E} . \tag{11}$$

In this equation it is necessary to clarify that the rate constant K is a global kinetic constant, different in principle from the K_D doublet rate constant given by Eq. (3), and obtained from the coagulation kinetic equation supposing that all the rate constants have the same values. In these conditions the evolution with time of the total number of aggregates, $N_T(E)$, is given by

$$\frac{dN_T}{dt} = -KN_T^2 \tag{12}$$

and also

$$\frac{N_j(E)}{N_0} = \frac{E^{j-1}}{(1+E)^{j+1}} . \tag{13}$$

Finally, introducing Eq. (8) in Eq. (10) it is easy to obtain

$$I_\theta(E) = I_\theta(0)\left[1 + 2\sum_{j=2}^{\infty} \frac{N_j(E)}{N_0} A(j,\theta)\right] . \tag{14}$$

Equation (14) represents the temporal evolution of the total intensity scattered at an angle θ.

If in Eq. (10) we only consider the initial time, where singlets and doublets cohabit, and evaluating $A(2,\theta)$ from Eq. (9) as

$$A(2,\theta) = \frac{\sin(2ah)}{2ah} , \tag{15}$$

where a is the particle radius and $h = (4\pi/\lambda)n_2\sin(\theta/2)$, it is direct to obtain [25]

$$\left[\frac{1}{I_\theta(0)}\frac{dI_\theta(E)}{dt}\right]_{t\to 0} = K_D N_0 \left(\frac{\sin 2ah}{2ah}\right) . \tag{16}$$

This equation permits the doublet rate constant K_D to be obtained from measurement of the initial slope of dispersed intensity versus time.

Experimental

Two polymer colloids having sulfonate and amine surface groups with dissimilar surface charge densities ($-3.6\ \mu C\,cm^{-2}$ and $+16.4\ \mu C\,cm^{-2}$, respectively) but equal particle sizes (370 ± 9 and 361 ± 5 nm) were used in the homocoagulation measurements. The anionic latex (SN4) and the cationic latex (M9) were synthesized following the recipes described in [30, 31], respectively. The surface charge densities and particle sizes were determined by conductimetric and potentiometric titrations, and by transmission electron microscopy (TEM), following the methods described in [32]. The polydispersity indexes (PDI, defined as D_w/D_n) for the latexes SN4 and M9 were 1.002 and 1.003, respectively, which confirms their monodispersity.

The electrokinetic data for the latexes were obtained with Zeta-sizer IV (Malvern Instruments, Malvern, UK). The electrophoretic mobility values were obtained by taking the average of six measurements, changing the sample suspension twice. The experimental error was taken as the standard deviation in these measurements, which was always below $\pm 0.2 \times 10^{-8}\ m^2\,V^{-1}\,s^{-1}$.

In turbidimetry, the rate constants were evaluated from the changes in absorbance with time in a Milton Roy Spectronic 601 instrument [33]. The spectrometer is connected to a computer which collects the data and calculates the initial slopes of the turbidity/time curves. The experiments were carried out by adding the electrolyte (0.6 ml) to the anionic or cationic particles (2.4 ml) redispersed in distilled water with a low ionic strength.

The aggregation process was also detected by nephelometric monitoring in a He–Ne laser nephelometer (wavelength of 633 nm) [34]. This nephelometer measures the light scattered at three different angles (5°, 10° and 20°). The injection into the cell was performed by simultaneous stopped flow mixing of two solutions, one formed by 1 ml of the particles redispersed in distilled water and low ionic strength, and the another by 1 ml of the solution at high ionic strength. The intensity of light scattered was measured immediately and its change versus time was collected by a computer. Curves were found to be linear in the early stages of coagulation at all electrolyte concentrations. The data treatment (calculation of intensity/time slopes and curves fitting) was made with a commercial computer program (ORIGIN 3.0).

Results and discussion

Latex characterization

The main characteristics of the SN4 and M9 latexes, as particle sizes and surface charge densities, were described in the experimental section. In this section the electrokinetic characterization and colloid stability of both latexes will be completed.

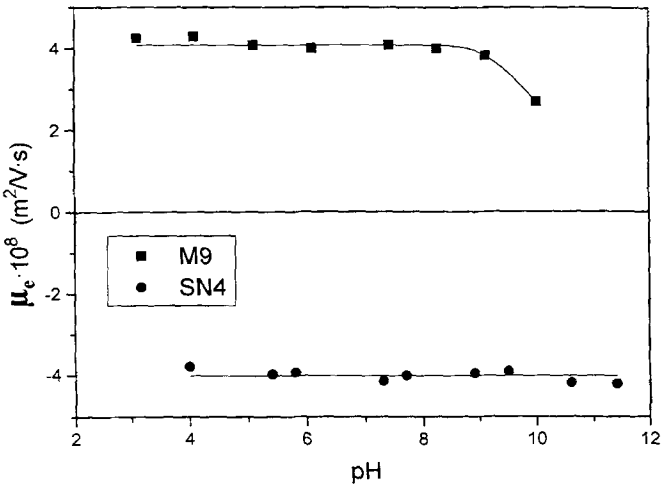

Fig. 1 Electrophoretic mobility of SN4 (●) and M9 (■) latexes versus the pH at an ionic strength of 0.001 M

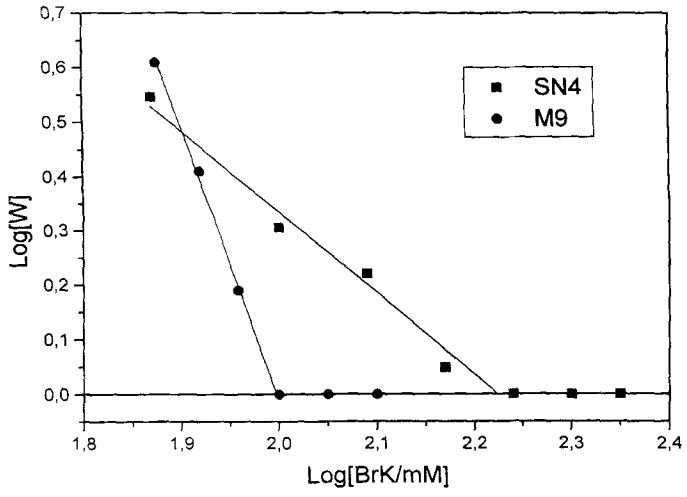

Fig. 2 Stability factor (W) versus the concentration of KBr for both latexes

Figure 1 shows the electrophoretic mobility (μ_e) of both latexes versus the pH, at constant ionic strength (0.001 M). The electrophoretic mobility μ_e is constant for the SN4 latex in the range 4–11, which confirms the strong acid character of the surface groups. However, the mobility of the M9 latex is pH-dependent decreasing at a pH higher than 9 and with coagulation appearing at higher pH. This result confirms the weak basic character of this latex as was previously obtained by conductimetric and potentiometric titration [35]. Therefore, we can modify the surface charge density of the M9 latex by changing the pH, and we had to control this factor to obtain reliable measurement with this latex.

To complete the characterization of the cationic and anionic latexes, we have studied the colloidal stability of each one against the addition of electrolyte (KBr). By using Eq. (1), from the plot of the stability factor versus electrolyte concentration, we have obtained the critical coagulation concentration (CCC) of both latexes, as shown in Fig. 2. The CCC was 0.175 M for the SN4 latex and 0.100 M for the M9 latex (pH 5.5). This data is very important because it permits us to establish the diffusion conditions for the next coagulation experiments.

Turbidimetric measurements

From homocoagulation experiments in turbidimetry, it is possible to estimate the doublet rate constant in diffusion conditions, $K_{D,F}$, for two latexes by using Eq. (2) and adding the appropriate ionic strength (above the CCC for each system). Figure 3 shows the $K_{D,F}$ values and the changes in the optical absorbance for the M9 latex vs. the

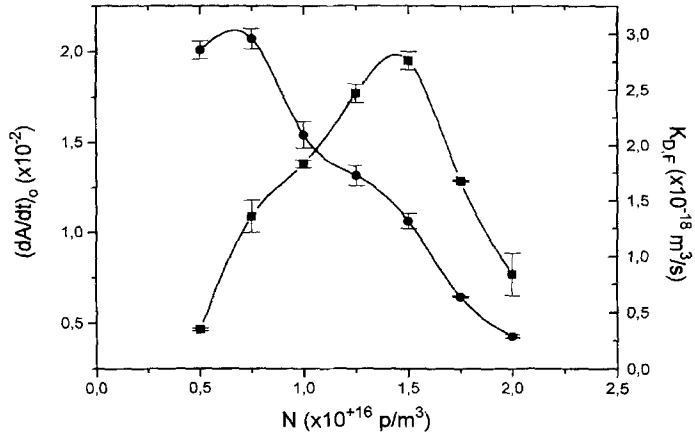

Fig. 3 Kinetic constant, $K_{D,F}$, (●) and change in the optical absorbance, $(dA/dt)_0$, (■) versus the particle concentration, N_0, for the M9 latex

initial particle concentration, N_0 (the wavelength, λ, was 600 nm and the added electrolyte concentration was 0.250 M KBr). As can be seen, $K_{D,F}$ was constant in a narrow range of N_0 and decreased when N_0 was higher than 0.8×10^{16} particles/m^3. The plateau value of $K_{D,F}$ is 2.8×10^{-18} particle m^3/s. In this figure the decrease of $K_{D,F}$ occurs even when the change in absorbance versus time, (dA/dt), presents a maximum. This fact was reported in a previous work [16] and successfully explained as a consequence of multiple light scattering which invalidated the results in the region below the plateau [35].

Figure 4 shows the $K_{D,F}$ values and the changes in the optical absorbance for the M9 latex vs. the wavelength (the initial particle concentration N_0 was 10^{16} particles/m^3 and

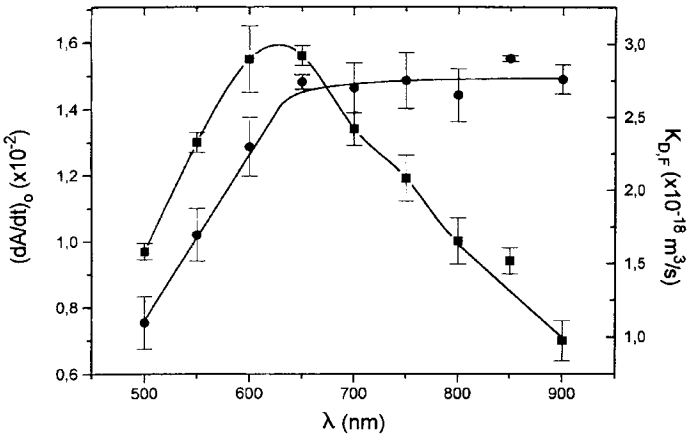

Fig. 4 Kinetic constant, $K_{D,F}$, (●) and change in the optical absorbance, $(dA/dt)_0$, (■) versus the wavelength ($N_0 = 10^6$ particle/m^3) for the M9 latex

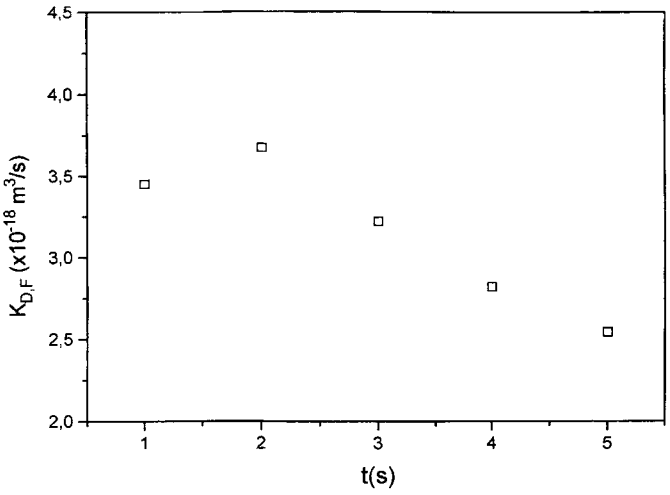

Fig. 5 Kinetic constant, $K_{D,F}$, versus the interval time used to calculate the initial slope of the $A(t)$ curve, for the M9 latex

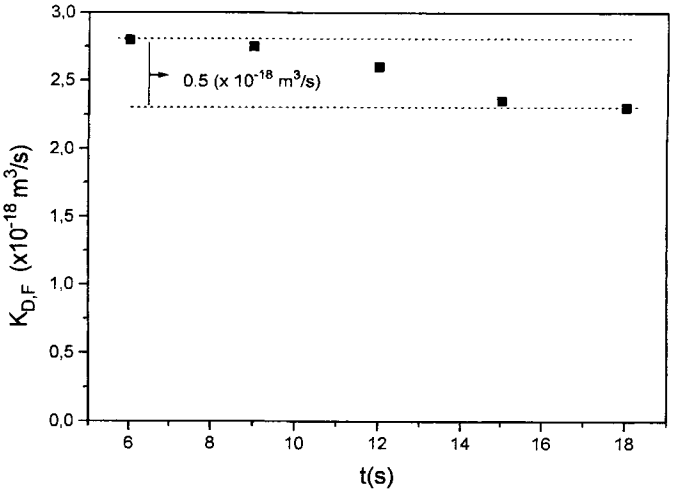

Fig. 6 Kinetic constant, $K_{D,F}$, versus the interval time used to fit the whole $A(t)$ curve, for the M9 latex

the added electrolyte concentration was 0.250 M KBr). We find that below a certain critical wavelength of 650 nm, there is not a similar value for the rate constant, while there is a plateau for wavelengths higher than the critical value. The average value of $K_{D,F}$ was 2.7×10^{-18} particles/m^3. This behavior has also been interpreted as multiple light scattering caused by the increase in the scattering sections of the doublet and singlet with the decreased wavelength [35]. However, we obtained the same value for the doublet rate constant in the diffuse conditions from the analysis of Figs. 3 and 4.

In the case of the anionic SN4 latex similar measurements were made and identical results were obtained in the two type of experiments for the doublet rate constant in diffuse conditions, with an average value of 2.7×10^{-18} particle m^3/s, just the same value found for the cationic system. Also, the analysis of the corresponding curves provided identical values for N_0 and λ critical, which is a direct consequence of the same size of both systems, although the latexes have different sign of the surface charge.

In order to eliminate arbitrary factors in the analysis of the data caused the manual drawing of the initial slopes, we decided to apply the fitting of the whole $A(t)$ curve method [27, 28] to obtain the doublet rate constant in diffusion conditions. Figure 5 shows the $K_{D,F}$ values obtained when several time intervals are used for drawing the initial slopes, appearing as a decrease in the kinetic constant for longer intervals. On the other hand, Fig. 6 shows the $K_{D,F}$ values obtained for longer times by using the fitting of the whole $A(t)$ curve method, with lower differences in the kinetic constant values. The reason for this difference is that little discontinuities in the $A(t)$ curve influence the drawing of initial slopes, but not in the fitting of the whole curve.

Finally, Fig. 7 shows the $K_{D,F}$ values versus the wavelength λ (N_0 was 10^{16} particle/m^3 and the added electrolyte concentration was 0.250 M KBr) for both latexes, obtained with the fitting of the whole $A(t)$ curve method. As can be seen, similar qualitative and quantitative results are obtained with low dispersion of the data, which permit us to rely on an experimental value of the doublet rate constant in diffusion conditions, $K_{D,F}$, of 2.75×10^{-18} particle m^3/s.

Nephelometric measurements

In analogy with turbidimetric runs, from homocoagulation experiments in nephelometry it is possible to estimate

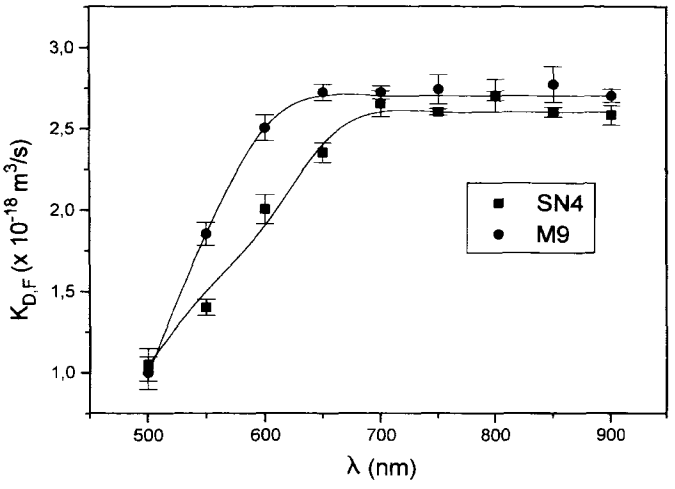

Fig. 7 Kinetic constant, $K_{D,F}$, versus the wavelength ($N_0 = 10^{16}$ particle/m^3) as calculated by fitting the whole $A(t)$ curve, for the SN4 (■) and M9 (●) latexes

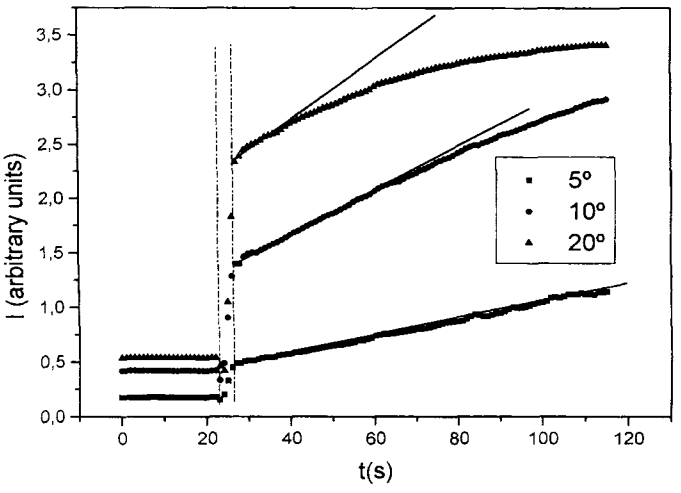

Fig. 9 Scattered light intensity at three different angles for the M9 latex at an ionic strength of 0.250 M

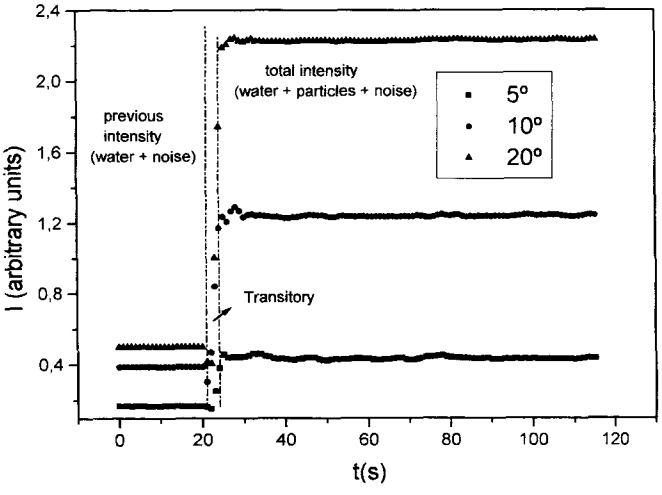

Fig. 8 Scattered light intensity at three different angles versus time for the SN4 latex at low ionic strength (without coagulation)

the doublet rate constant diffusion conditions, $K_{D,F}$, for both latexes by using Eq. (16) and adding the appropriate ionic strength (above CCC for each system). The total rate constant in diffusion conditions, K_F, can also be calculated for both latexes by using Eq. (14) in the same conditions. The difference consists only in the data treatment method, but not in the practical measurements. The first case is based in the drawing of initial slopes, and the second one, in the fitting of the whole curve.

However, both data treatments require to obtain the scattered intensity at zero time $I_\theta(0)$. That parameter is shown in Fig. 8 for the latex SN4. This value can be obtained in practice by injecting distilled water in the cell (with a negligible ionic strength), which prevent any further coagulation process. Also, it can be seen that the scattered light increases with the scattering angle. In particular, it is clear that the scattered intensity at 5° is similar to the noise intensity, which could invalid the results obtained for this angle.

Figure 9 shows a typical run for the latex M9 and ionic strength of 0.250 M (KBr). It is clear a linear dependence for the angle of 5°, and also a wide time interval of linearity for 10°, which give an unambiguous drawing of the initial slope. That does not occur for the 20° angle. However, we could obtain the doublet rate constants by using this angle also.

In the case of fitting of the whole curve by the $I_\theta(t)$ method, we chose to eliminate the 20° angle, owing to the high dependence of the form factors with the (unknown) geometry of the aggregates [22] and having in mind that these differences increase with the scattering angle. Also, it is necessary to clarify that in the fitting treatment we consider the presence of aggregates formed up to 13 monomers, and that we used the proposed formulae in ref. [22].

Figure 10 shows the doublet rate constant in diffusion conditions versus the initial particle concentration in the cell, for the three studied angles and for the latex M9, calculated by the drawn of initial slopes. As can be seen, for the two major angles (10° and 20°) and for a particle concentration below 0.5×10^{16} particle/m^3, the results are in agreement with the average value of 2.75×10^{-18} particle m^3/s, obtained by turbidity. Random values were found for the angle of 5° and also for the other two angles when the particle concentration was above the mentioned critical value. This behavior has been interpreted as a consequence of the multiple dispersion in analogy with the reported turbidimetric results [16], and we have only considered the results concerning the low particle

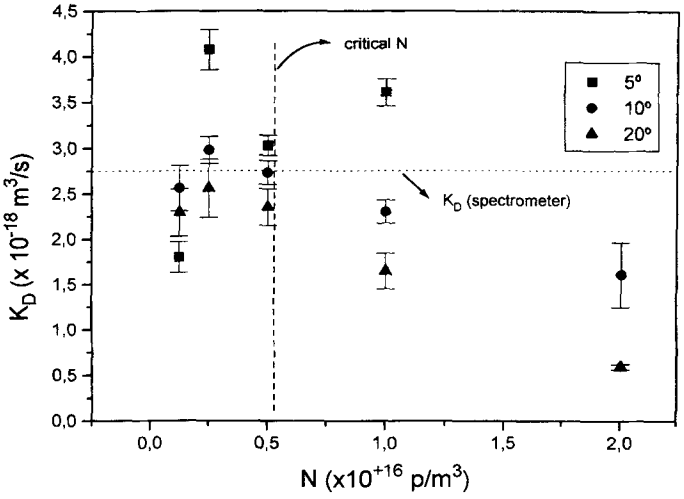

Fig. 10 Doublet kinetic constant, K_D, versus the particle concentration for the M9 latex and three different angles [(■) 5°; (●) 10°, and (▲) 20°], as calculated by the initial slopes of the $I(t)$ curves

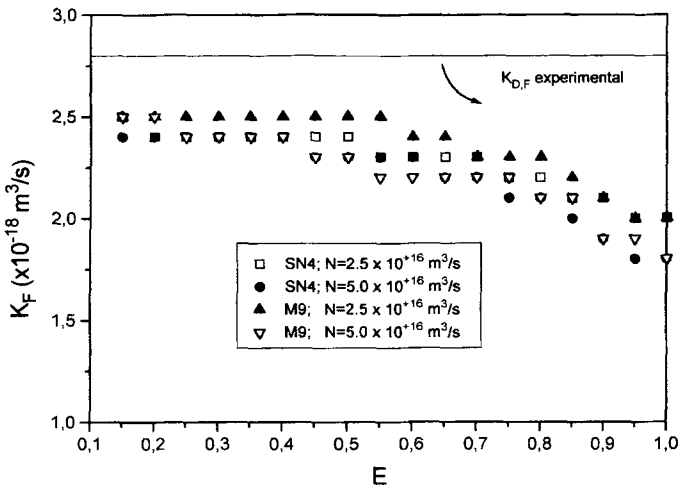

Fig. 11 Global kinetic constant, K_F, versus the nondimensional time, E, for both latexes and two particle concentrations, as obtained by nephelometry

concentrations and for the angles of 10° and 20°. Similar results were found for the latex SN4, which permits us to establish an experimental value for the doublet rate constant "in diffusion conditions" of 2.75×10^{-18} particle m^3/s.

The global rate constant in diffusion conditions, K_F, can be determined by using the same experimental data. So, for each nondimensional time value, E (defined by Eq. (11)), we select the magnitude of K_F that fits the theoretical value of the total scattered intensity $I_\theta(E)$ provided by Eq. (14). This method [22] permits us to plot the K_F rate constant versus the nondimensional time E. Figure 11 shows the K_F values for the two latexes and the two selected particle concentration of 0.25×10^{16} and 0.50×10^{16} particle/m^3. We obtain, for all cases, a constant value of K_F between 2.4×10^{-18} and 2.5×10^{-18} particle m^3/s for E values below 0.55. K_F decreases for larger values of E, which must be interpreted as a direct consequence of the increasing scattering of the larger aggregates. The analysis of Fig. 11 supports this hypothesis' showing that the critical value of E that limits the two regions (plateau and decreasing zone) is N_0-dependent, decreasing with increase in the initial particle concentration N_0.

Finally, we have found dissimilar values for $K_{D,F}$ and K_F, which admits a clear explanation: the rate constant K_F characterizes the global coagulation process of a colloidal dispersion, and it is different to the $K_{D,F}$ rate constant that characterizes the double formation process.

Conclusions

An unambiguous experimental value for the doublet rate constant in diffusion conditions $K_{D,F}$ is obtained by using the turbidimetric and nephelometric techniques. By turbidity measurements, using the fitting method of the whole $A(t)$ curve reliable values of the kinetic constant have been obtained. These data showed lower dispersion than those obtained by using the initial slopes and are in agreement with those obtained by nephelometry experiments. The accordance between the different experimental data has permitted us to establish a value for the $K_{D,F}$ rate constant of 2.75×10^{-18} particle m^3/s, equal for both latexes. By nephelometry both data treatment methods have permitted us to distinguish between the doublet rate constant in diffusion conditions $K_{D,F}$ and the global rate constant in diffusion conditions K_F. For the K_F rate constant a value between 2.4×10^{-8}–2.5×10^{-18} particle m^3/s was obtained, equal for both latexes.

Acknowledgements The financial support provided by CICYT (under Project MAT96-1035-C03-03) is greatly appreciated. The authors wish to express their gratitude to Dr. Delfi Bastos and Dr. Curro Galisteo for synthesizing the latexes used throughout this work.

References

1. Derjaguin BV, Landau L (1941) Acta Physicochim URSS 14:633
2. Verwey EJW, Overbeek JThG (1948) Theory of the Stability of Lyophobic Colloids, Elsevier, New York
3. Bleier A (1992) Colloids Surfaces 66:157
4. Miao X, Marquis PM (1992) Nanostructured Mater 1:31

5. Wang Q (1992) J Colloid Interface Sci 150:418
6. Vincent B, Young CA, Tadros ThF (1978) J Chem Soc Faraday Trans 65:296
7. McLaughlin WJ, White JL, Hem SL (1993) J Colloid Interface Sci 157:113
8. Peula JM, Hidalgo-Alvarez R, Santos R, Forcada J, de las Nieves FJ (1995) J Mater Sci: Mater Medicine 6:779
9. Peula JM, Hidalgo-Alvarez R, de las Nieves FJ (1995) J Biomater Sci Polym Ed 7:231 and 7:241
10. Okubo M, Miyachi N, Lu Y (1994) Colloid Polym Sci 272:270
11. Sonntag H, Strenge K (1987) Coagulation Kinetics and Structure Formation, Plenum, New York
12. Swift DL, Friendlander SK (1964) J Colloid Interface Sci 19:621
13. Matthews BA, Rhodes CT (1970) J Colloid Interface Sci 32:332
14. Pelssers EGM, Cohen Stuart MA, Fleer GJ (1990) J Colloid Interface Sci 137:350
15. Lichtenbelt JWTh, Pathmamanoharan C, Wiersema J (1974) J Colloid Interface Sci 49:281
16. Maroto JA, de las Nieves FJ (1995) Colloids Surfaces A 96:121
17. Maroto JA, de las Nieves FJ (1995) Prog Colloid Polym Sci 98:89
18. Novich BE, Ring TA (1984) Clays Clay Miner 32:400
19. Barringer EA, Novich BE, Ring TA (1984) J Colloid Interface Sci 2:584
20. Herrington TM, Midmore BR (1989) J Chem Soc Faraday Trans I 85:3529
21. Virden JW, Berg JC (1992) J Colloid Interface Sci 149:528
22. Lips A, Smart C, Willis E (1971) J Chem Soc Faraday Trans I 67:2979
23. Lips A, Willis E (1973) J Chem Soc Faraday Trans I 69:1226
24. Giles D, Lips A (1978) J Chem Soc Faraday Trans I 74:733
25. van Zanten JH, Elimelech M (1992) J Colloid Interface Sci 154:1
26. Islam AM, Chowdry BZ, Snowden MJ (1995) Adv Colloid Interface Sci 62:109
27. Maroto JA, de las Nieves FJ (1996) Anal Física 92:3
28. Puertas AM, Maroto JA, de las Nieves FJ (1997) Colloid Surfaces, accepted for publication
29. Lips A, Levine S (1970) J Colloid Interface Sci 33:455
30. de las Nieves FJ, Daniels ES, El-Aasser MS (1991) Colloids Surfaces 60:107
31. Hidalgo Alvarez R, de las Nieves FJ, van der Linde AJ, Bijsterbosch BH (1986) Colloids Surfaces 21:259
32. Bastos D, de las Nieves FJ (1993) Colloid Polym Sci 271:860
33. Rubio-Hernández FJ, de las Nieves FJ, Hidalgo-Alvarez R, Bijsterbosch BH (1994) J Dispersion Sci Tech 15:1
34. Sarobe J, Miraballes I, Molina JA, Forcada J, Hidalgo-Alvarez R (1996) Polym Adv Technol 7:749
35. Maroto JA, de las Nieves FJ, Colloids Surfaces, accepted for publication